RSC Advances

ROYAL SOCIETY OF CHEMISTRY

www.rsc.org/advances

Journal Name

RSCPublishing

ARTICLE

Remarkable enhancement of ambient-air electrical conductivity of the perylenediimide π-stacks isolated in the flexible films of a hydrogen-bonded polymer†

Cite this: DOI: 10.1039/x0xx00000x

Received 00th January 2012,
Accepted 00th January 2012

DOI: 10.1039/x0xx00000x

www.rsc.org/

Mustafa Supur,*[a] Ayhan Yurtsever[bc] and Ümit Akbey[def]

N,*N'*-di(2-(trimethylammoniumiodide)ethylene) perylenediimide (TAIPDI), forming extensive π-stacks through the strong π-π interactions of large π-planes, was isolated in the hydrogen-bonding milieu of polyvinyl alcohol (PVA) from aqueous solutions. The stacking behaviour of TAIPDIs in PVA films was investigated by using UV-vis and magic angle spinning nuclear magnetic resonance (MAS NMR) spectroscopy. It was concluded that the TAIPDI molecules organized as extensive π-stacks in the PVA matrix controlled by the interactions with the polymer chains. The resulting films of TAIPDI/PVA were doped with electrons by using a strong reducing agent. The electrical current obtained in the electron-doped TAIPDI/PVA films was 740 times higher under the same bias as compared to that of reduced TAIPDIs casted on a glass substrate without a polymer additive. The significant increase in the conductivity of electron-doped TAIPDI/PVA films reflects the strong effect of the uninterrupted π-stacking of TAIPDIs extending in the flexible PVA films and the protection of the doped electrons from the oxygen in the air, provided by the H-bonded environment in PVA.

Introduction

Self-assembly of suitable organic molecules stimulates the construction of new supramolecular materials with unique functional characteristics to be employed in the optoelectronic devices.[1] In this regard, self-assembled structures of perylenediimides (PDIs) continue to draw much attention.[2] Besides their remarkable spectral and electrochemical properties, PDIs stand out with the high chemical, thermal and photostability. Self-organizations of large π-planes of electron deficient PDIs through the strong π-π interactions yields electron-transport conduits extending in one dimension (1D) at nanoscale.[3] Electron transport in these extensive π-stacks is realized by the intermolecular π-electron migration, in which the π-electrons (e.g. PDI radical anions) are generated via a thermal or a photoinduced electron-transfer process from electron-donating species (electron doping).[4] Extensive π-electron transport in these nanostructured organizations significantly improves the (photo)conductivity.[5] Nonetheless, the electron transport as well as the electrical conductivity observed in the PDI conduits is heavily retarded by O_2 molecules in the air, which oxidize the PDI anions ($PDI^{\bullet-}$) to yield superoxide (O_2^{-}).[6] In addition to this, PDI nanofibrils are mostly brittle and exhibit fractures in the solid state,[4c,5b,7] which makes them susceptible to the impacts and bending. Such fractures interrupt the continuous mobility of electrons through the PDI stacks, thereby reducing the conductivity under an applied bias.

To address the stated limitations of the current PDI fibrils, we isolated the π-stacks of a water-soluble PDI (*N*,*N*'-di(2-(trimethylammonium iodide) ethylene) perylenediimide, TAIPDI, Fig. 1) in the flexible films of polyvinyl alcohol (PVA). TAIPDI molecules form extensive π-stacks in water through the strong π-π interactions of the hydrophobic large π-planes.[4c,d,8] 1D nanostructures of π-stacked TAIPDIs were obtained from their aqueous solutions when casted on a substrate as monitored by the scanning electron microscopic tools.[4c,8] PVA is a promising template for the isolation of the self-assembled PDIs from their aqueous solutions because of its hydrogen-bonded matrix formed by –OH groups.[9] PVA films reveal significant flexibility[10] as a result of a such H-bonding environment, in which the brittleness and cracks of TAIPDI stacks can be effectively minimized. H-bonded textures of polymers are acknowledged for the minimum porosity, which drastically reduce the permeability of gas molecules from air.[11] Films of water-soluble vinyl polymers with small substituents, feasible for H-bonding, are also known to be less porous compared to those having large, rigid substituents, such as pyrrolidone groups.[12] Therefore, PVA films with reasonable elasticity can be employed to protect the reduced PDI stacks from the oxygen at ambient conditions. In addition, the utilization of water for dissolving the PVA and TAIPDI stacks

during the isolation process is advantageous for environmentally benign large-scale fabrication.

PVA was previously used to cast the flexible and conductive films of polytetrathiooxalate, naphthalenediimide, and tetrathiafulvalene.[13] Nonetheless, comprehensive information about the effect of the PVA matrix on the stacking behaviour of the aromatic structures as well as the comparison with different polymer environments to understand the effect of H-bonding on the *I-V* characteristics were lacking in these studies.

The isolation of PDIs in the different polymer matrices has been a current subject of various research fields. In a recent report, in which a PDI derivative was isolated in vinyl alcohol polymers, the effect of temperature and chemical environment on the extent of embedded PDI aggregates and the sensitivity of these aggregates towards the mechanical stress were investigated.[14] In another study, PVA was incorporated as a polar polymer dielectric in a PDI-based organic field effect transistor.[15] The immobilised PDI entities on PVA chains through the esterification were demonstrated as promising fluorescent labels for biologically active probes.[16] PDIs were also covalently and non-covalently isolated in various polymer and oligomer environments to investigate their aggregation behaviours and emission spectral characteristics for various purposes.[17] However, the investigations on the electrical conductivity of electron-doped PDI aggregates isolated in polymer films have been missing so far.

In this study, the impact of the PVA chains on the organizations of π-stacks of TAIPDIs extending in the polymer films were extensively examined by UV-vis and magic angle spinning nuclear magnetic resonance (MAS NMR) spectroscopy. Reduced TAIPDIs, i.e. TAIPDI anions, in the films were detected by UV-vis spectroscopy and confirmed by electron paramagnetic resonance (EPR) spectroscopy. *I-V* characteristics of reduced TAIPDIs drop-casted on a glass without any polymer and those isolated in PVA films were compared at ambient air conditions. *I-V* curves of reduced TAIPDIs were also obtained in a non-H-bonding polymer (polyvinyl pyrrolidone, PVP) to understand the effect of different polymer environment on the electrical conductivity.

Results and discussion

Fabrication of TAIPDI/PVA films and UV-Vis spectral characteristics of neutral TAIPDI stacks in PVA films

The isolation of TAIPDIs in PVA was achieved by mixing aqueous solutions of TAIPDIs and PVA (10 mg ml^{-1}) at room temperature. The TAIPDI/PVA solutions with different TAIPDI contents were then cast into glass Petri dishes to dry at 60ºC in an oven for overnight. After drying, the resulting films were kept at 110ºC for about 2 hours for further removal of water. The resulting films were easy to process and displayed reasonable flexibility (Fig. 1 and Fig. S1, ESI). Thickness of the prepared films was about 2–5 μm, which depends on the amount of TAIPDI/PVA solution in the Petri dishes.

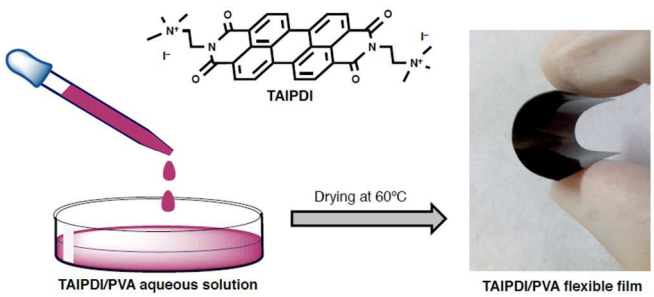

Fig. 1 The molecular structure of TAIPDI and the fabrication of TAIPDI/PVA flexible films from aqueous solutions. The photographic image shows the flexibility of the PVA film with 30 wt.% TAIPDI content.

Absorption spectra of TAIPDI in PVA films vary with the concentration (Fig. 2).[18] At low concentrations of TAIPDI dispersed in PVA matrices (2.0 and 3.3 wt.%), the 0–0, 0–1, and 0–3 transitions were observed at 535, 501, and 473 nm, respectively. The ratios of 0–0 to 0–1 transitions were calculated to be 1.05 and 0.84 for 2.0 and 3.3 wt.%, respectively, whereas it was estimated to be 1.48 in MeOH solution, in which TAIPDI molecules were completely dissolved at room temperature.[4c] Besides the low ratios of 0–0 to 0–1 transitions, the small red shift and a meaningful broadening at around 570 nm were noted when the concentration of TAIPDI was increased from 2.0 to 3.3 wt.%. These features indicate that π-stacking between the TAIPDI planes are considerably effective at low concentrations in these polymer environments. As the dispersion of TAIPDI in PVA was increased to 10 wt%, the vibronic transitions, the reminiscent of the monomeric identity, were completely replaced by an absorption peaking at 503 nm with a small shoulder around 535 nm, which resembles to that of TAIPDIs in aqueous environments, in which cofacial stacking [$(TAIPDI)_n$] was observed as a result of hydrophobic π-π interactions.[4c] Nonetheless, the absorption band of $(TAIPDI)_n$ in PVA was broader and less featured compared to that in water. In addition, the shoulder around 535 nm appeared at 565 nm in the absorption spectrum of TAIPDIs cast on a glass substrate from aqueous solution without PVA (Fig. S2, ESI). Hence, the TAIPDI molecules organize as extensive π-stacks in the PVA matrix governed by the interactions with the

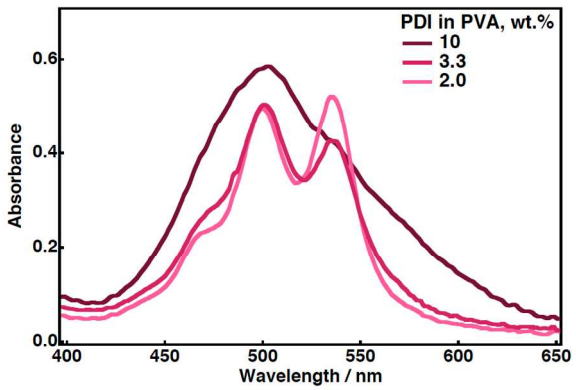

Fig. 2 Absorption spectra of neutral $(TAIPDI)_n$ in PVA films at indicated weight ratios.

polymer chains. The absorption features of the TAIPDI/PVA did not show any change after the their preparation indicating their stability.

Investigation of self-organizations of neutral TAIPDI stacks in PVA films *via* ^{1}H MAS NMR spectroscopy

To understand the supramolecular interactions (hydrogen bonding and π-π packing) of TAIPDIs and PVA, we performed solid-state ^{1}H MAS NMR experiments. Proton NMR spectroscopy has been shown to be very informative to understand molecular interactions and proton chemical information.[19] Such information gives the hint on local packing of TAIPDIs and how that changes with the interaction via PVA.[20] Moreover, the ^{1}H double-quantum (DQ) MAS NMR experiments give further information on spatial proximities of protons that can reveal the details of packing and hydrogen bonding.

The proton chemical resonances observed for four different samples are shown in Fig. 3. Pure PVA has characteristic CH_2 and CH NMR peaks from polymer backbone and additional –OH shoulder (~5-6 ppm, Fig. 3b). The pure TAIPDI has CH_2/CH_3 resonances at ~4 ppm and the aromatic ring protons between 6-9 ppm range. Only one resonance is expected from the similar ring protons (marked with a solid line in Fig. 3b), that is at 8.50-8.95 ppm in a DMSO-d_6 solution (Fig S3, ESI). However, we observed four different chemical shifts for the solid TAIPDI sample (H_1-H_4). This observation indicates that there is differential ring-current affects observed by different ring protons, namely with four different strength, and as a result, a shift is observed towards lower proton chemical shifts as the ring-current effect becomes stronger. Such phenomenon is observed in materials forming packed aromatic arrays.[19g]

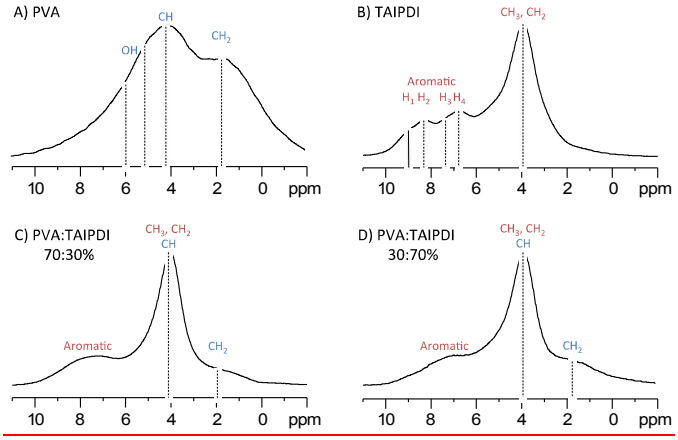

Fig. 3 ^{1}H double-quantum filtered (DQF) MAS NMR spectra of (a) PVA, (b) TAIPDI, (c) PVA:TAIPDI 70:30% and (d) PVA:TAIPDI 30:70% samples. Spectra were recorded with one rotor-period of DQ excitation/reconversion and at ambient temperatures, 50 kHz MAS, and 700 MHz Bruker NMR spectrometer. Assignment of proton resonances to various chemical sites is represented along with the spectra with dashed lines. The –OH ^{1}H chemical shift position is shown for the PVA sample with dotted lines (~5-6 ppm) in Fig 3a. The solid line at the ^{1}H spectrum in Fig. 3b additionally indicates the chemical shift position of the aromatic protons (~8.7-9 ppm) of PDI recorded in DMSO (Fig. S3, ESI).

Upon the mixing of PVA and TAIPDI, those four distinct aromatic proton resonances were replaced by a less featured aromatic region (Fig. 3c-d).

To delve further into the aromatic proton chemical shifts and packing arrangements, we recorded the 2D ^{1}H-^{1}H DQ MAS NMR spectra of the samples as shown in Fig. 4. In these spectra, due to the increased resolution in the second DQ dimension (the y-axes of the spectra), different aromatic proton resonances can be identified. PVA has the characteristic CH and CH_2 auto ^{1}H-^{1}H cross-peaks at the diagonal. Moreover, two additional auto cross peaks can be monitored at ~5 and ~6 ppm, that were assigned to inter and intra hydrogen bonded –OH protons, respectively (Fig. 4a).[9] For the pure TAIPDI, the H_1 aromatic proton has a chemical shift similar to the solution state at ~8.9-9 ppm, which indicates a very weak or no ring-current effects on this proton type (Fig. 4b). Then, from H_2 towards H_4, the ring current effects become larger; as a result, the resonances shift away from the solution chemical shift towards the lower values. H_4 is at ~6.5 ppm, which undergoes the largest ring-current effect from the stacked TAIPDI molecules. Remarkably, when TAIPDI and PVA is mixed with two different ratios, the H_1 proton resonance disappears from the spectra, indicating the removal of the aromatic proton experiencing no ring-current effects (Fig. 4c-d). This observation reveals the stronger stacking of the TAIPDI π-planes in the PVA/TAIPDI mixtures as compared to those of pure TAIPDIs, as confirmed by the UV-Vis spectral experiments (Fig. 2). It is also possible that the arrangement of the TAIPDI is changed in a way that leads to a more complex and involved packing, *via* more TAIPDI fibre stacks interacting

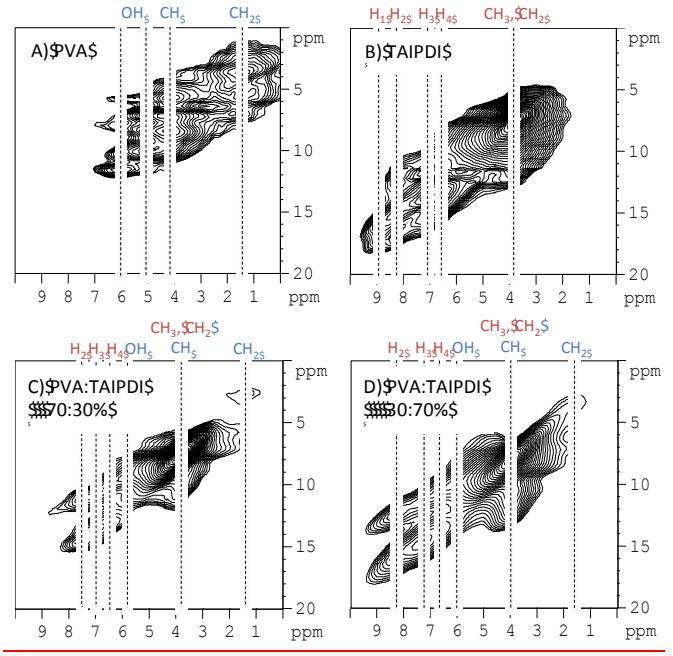

Fig. 4 The 2D ^{1}H-^{1}H DQ MAS NMR spectra of (a) PVA, (b) TAIPDI, (c) PVA:TAIPDI 70:30% and (d) PVA:TAIPDI 30:70% samples. Spectra were recorded with one rotor-period of DQ excitation-reconversion and at ambient temperatures, 50 kHz MAS, and 700 MHz Bruker NMR spectrometer. The proton chemical shift assignments are noted in the corresponding figure.

with each other. Moreover, the NMR cross-peak pattern observed for the mixtures are much less featured compared to the pure TAIPDI, as a result of a possible more dynamic or less ordered arrangement of the stacks. The H_2, H_3 and H_4 types of protons are all still exist in the mixtures, with slight chemical shift changes. The –OH peaks are still partly observed in the mixture samples, as seen as a cross peak at ~5-6 ppm.

UV-Vis spectral characteristics of reduced TAIPDI stacks in PVA films

TAIPDI stacks isolated in PVA can be reduced by using a strong electron dopant, hydrazine vapour. Efficient electron transfer from electron-donating hydrazine to the electron-accepting PDIs is feasible as observed in previous studies.[4b,c,5b] As expected, 30 seconds of exposure of PVA film containing 2.0 wt.% of TAIPDI to hydrazine vapour at ~60ºC resulted in the formation of radical anion of TAIPDI ($TAIPDI^{\bullet-}$) as recognized from the absorption appeared at around 710 and 800 nm (Fig. 5a).[21] These absorption peaks became more apparent as the exposure time to hydrazine vapour was increased. Further hydrazine exposure caused the reduction of the majority of the radical anions to the dianions of TAIPDI ($TAIPDI^{2-}$) as noted from the gradual decrease in the absorption peaks at 710 and 800 nm, which was followed by the instant rise at 520, 545 and 626 nm.[22]

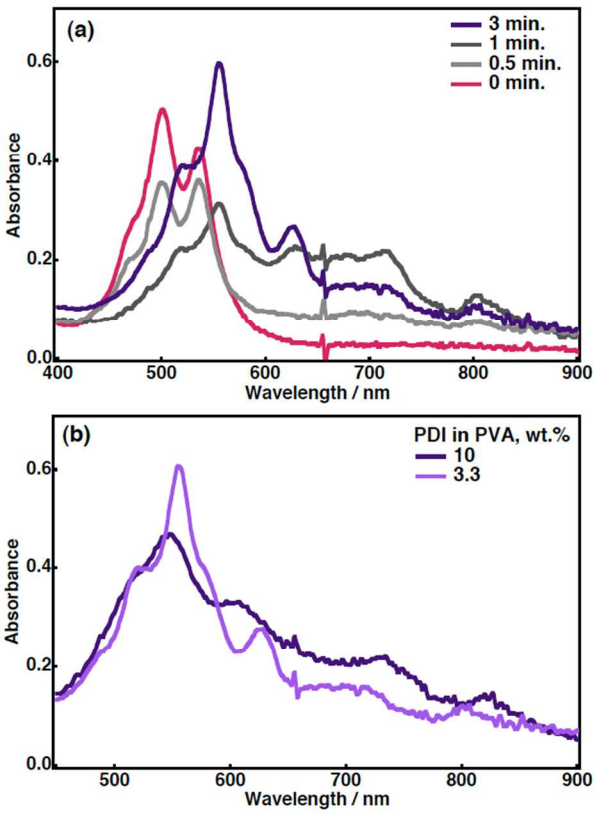

Fig. 5 (a) Absorption spectra showing the reduction of TAIPDIs in PVA films (3.3 wt.%) at indicated exposure times to hydrazine vapour at 60°C. (b) Absorption spectra of reduced TAIPDIs in PVA films at indicated weight ratios.

The increase in the weight percent of TAIPDI in PVA (10 wt.%) led to red shift in the absorption bands of $TAIPDI^{\bullet-}$ to 734 and 825 nm while those of $TAIPDI^{2-}$ revealed blue shift to 514, 536 and 606 nm (Fig. 5b). This results from the enhanced π-stacking among the TAIPDI molecules in the PVA film. The absorption maxima of $TAIDPI^{\bullet-}$ with 3.3 and 10 wt.% in PVA mainly corresponded to those of PDI radical anions obtained in ethanol and water, respectively.[23] Nonetheless, the absorption features of $TAIPDI^{2-}$ with 3.3 and 10 wt.% in PVA were red shifted compared to those of PDI dianions obtained in ethanol and water.[23] Reduced species of TAIPDI, i.e. $TAIPDI^{\bullet-}$ and $TAIPDI^{2-}$, isolated in PVA films can be recognized from the violet colour of the films while the neutral TAIPDI gives red colour. The complete colour change from violet to red takes about a month, indicating the effect of the isolation in PVA matrix on the stability of the reduced TAIPDIs.

The effect of H-bonding surrounding the TAIPDI stacks on the lifetime of the reduced species of TAIPDI was tested by a comparison with a non-H-bonding environment in the ambient air. For this purpose, TAIPDI was isolated in PVP (3.3 wt.%) by repeating the same procedures for the fabrication of the PVA films and exposed to the hydrazine vapour at ~60ºC. After 3 minutes of exposure, the reduced TAIPDI in PVP films were spectroscopically compared with those in PVA. The absorption spectrum of the reduced species of TAIPDI in PVP differed from that of PVA film (3.3 wt.%) by significant shifts as a result of the interactions with the pyrrolidones instead of –OH groups (Fig. S6, ESI). Other than the spectral shifts, the lifetime of the reduced species of TAIPDI in PVA was much longer than those in PVP. As shown, in Fig. 6, two third of the reduced TAIPDIs in PVP decomposes within 1.5 hr whereas no significant decay for those isolated in PVA was detected during the course of the measurement (ca. 17 hrs).[24] The stability of the reduced species in PVA can be related to the air permeability, which is probably minimized *via* the H-bonding matrix among the –OH groups.[11] On the other hand, the rigid pyrrolidones are most likely to enhance the porosity of the polymer film, which relatively favours the air permeation into the PVP bulk.[12]

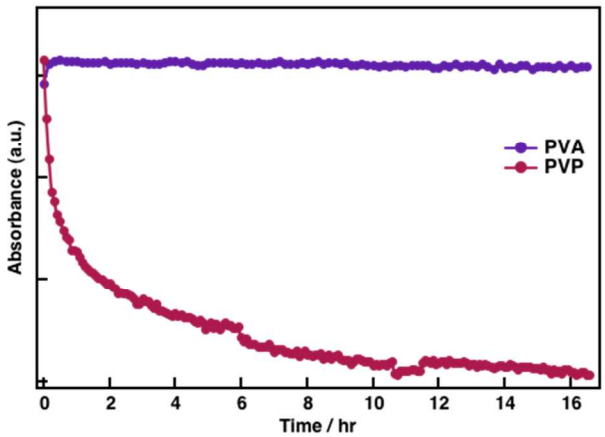

Fig. 6 Time profile at 640 nm showing the decay of the reduced species of TAIPDI (3.3 wt.%) in PVA and PVP films in ambient air.

I-V characteristics of reduced TAIPDI stacks in PVA films

To reveal the *I-V* characteristics of TAIPDI/PVA films, aqueous solution of TAIPDI and PVA was drop-casted on a glass substrate to form film spots (10 and 30 wt.% TAIPDI) with an area of 20 mm^2 and a thickness of 2–5 μm after drying. These film spots were exposed to hydrazine vapour to obtain reduced TAIPDIs (electron-doped). Two tungsten electrodes with a diameter of 10 μm were used to obtain *I-V* curves on the corresponding TAIPDI/PVA films at room temperature. Under applied bias of 5.0 V, PVA film containing 30 wt.% TAIPDI displayed a current of 260 nA at ambient conditions. On the other hand, TAIPDI aggregates casted from aqueous solution onto a glass substrate without any polymer protection gave only 0.35 nA under the same bias at the same conditions (Fig. 7a).[25] 740-fold increase in the current reveals the strong effect of the self-organization of TAIPDIs through the tight stacking in PVA films and the protection of the doped electrons from oxygen in the air. Soft H-bonding texture of PVA also prevents the fractures of TAIPDI stacks, which provides a continuous electron flow. From the linear *I-V* curve, the conductivity of the PVA film was roughly estimated to be 0.035 S m^{-1}.[26] As the TAIPDI content decreased to 10 wt.% in PVA film (Fig. 7b), the current under 5.0 V bias reduced about 90 % (28 nA). π-stacking among the TAIPDIs were significantly improved as the concentration of TAIPDI was increased (Fig. 2). Hence, the long-range migration of doped electrons along the extensive π-stacks of TAIPDIs embedded in the PVA matrix is necessary to obtain high electrical conductivity on these films.

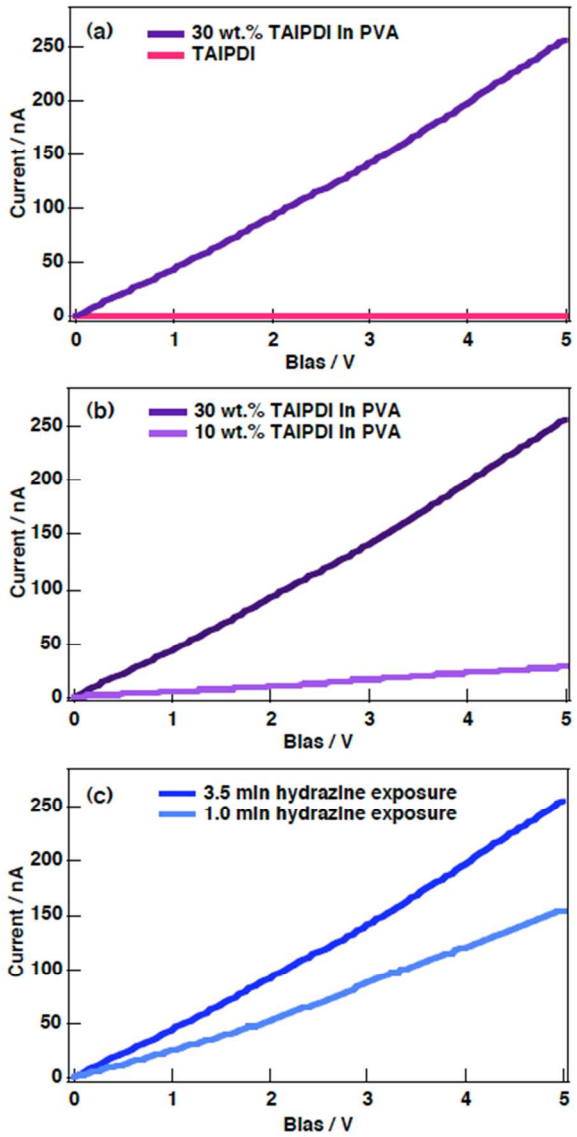

Fig. 7 (a) *I-V* curves of reduced TAIPDI (30 wt.%) in PVA and reduced TAIPDI without polymer isolation, (b) *I-V* curves of reduced TAIPDI in PVA at indicated weight percents and (c) *I-V* curves of reduced TAIPDI (30 wt.%) in PVA with indicated exposure times to hydrazine vapour.

It was also found that the amount of doped electrons migrating on the TAIPDI π-stacks controls the electronic conductivity. The PVA film with 30 wt.% TAIPDI subjected to hydrazine vapour 3.5 minutes showed 1.7 times higher current as compared to that subjected to hydrazine only 1.0 minute under the same bias (Fig. 7c).

Furthermore, the electrical conductivities of reduced TAIPDIs isolated in PVA and PVP were compared to understanding the effect of H-bonding. TAIPDI/PVP film spots were obtained on a glass substrate by applying the same procedure for TAIPDI/PVA films. PVP film with 30 wt.% TAIPDI displayed a current of 190 nA at ambient conditions. Nonetheless, it drastically dropped to 12 nA after two hours while the current obtained from PVA films was steady within the same time course (Fig. S8, ESI). *I-V* characteristics of PVA and PVP films of TAIPDI are in agreement with the lifetimes of the reduced TAIPDIs isolated in the films of corresponding polymers (Fig. 6).

Conclusions

In conclusion, extensive TAIPDI π-stacks were isolated in the PVA films. H-bonding matrix of PVA provides flexibility for TAIPDI stacks and restricts the oxidation of reduced TAIPDIs by O_2 molecules in the air. TAIPDI stacks rearrange in the PVA films as a result of interactions with the polymer chains, as seen in the NMR results. By this way, TAIPDI π-stacks extend uninterruptedly with the help of PVA chains. H-bonded environment of PVA drastically improves the electrical conductivity realizing in the TAIPDI π-stacks, which is 740 times higher compared to that of pure TAIPDI without polymer film. The electrical current obtained from the reduced TAIPDIs isolated in H-bonding matrix is much more stable as compared to that of isolated in non-H-bonding polymer. Such improvement can facilitate the use of PDI/polymer films as conductive interfacial layers in the organic optoelectronic devices.

Experimental

Materials

N,*N*'-di(2-(trimethylammonium iodide) ethylene) perylene diimide (TAIPDI) was synthesized according to the reported procedures.[4c] Polyvinyl alcohol (PVA; average Mw: 85000-124000, Sigma-Aldrich), polyvinylpyrrolidone (PVP K30; average Mw: 40000, TCI or Nacalai Tesque) and hydrazine anhydrous (TCI) were used as received from commercial sources. *Caution: Anhydrous hydrazine reacts violently with many metals, metal oxides and porous materials causing fire and explosion. Exposing to heat, flame or oxidising agents can cause fire hazard*. Purification of water (18.2 MΩ cm) was performed with a Milli-Q system (Millipore, Direct-Q 3 UV).

Instruments

Steady-state absorption measurements were recorded on a Hewlett Packard 8453 diode array spectrophotometer. Solid-state MAS NMR measurements were performed at a 700 MHz Bruker instrument, equipped with 1.3 mm HCN triple-resonance probe, at room temperature and 50 kHz MAS. Electron paramagnetic resonance (EPR) spectra were taken on a JEOL X-band spectrometer (JES-RE1XE) at room temperature. *I-V* characterization of films was done on an Agilent Technologies B1500A semiconductor device analyzer with B1510A precision high power source measurement unit.

Acknowledgements

M.S. thanks JSPS for a fellowship and Professor Shunichi Fukuzumi for his helpful suggestions. U.A. acknowledges financial support from DFF Mobilex grant and AIAS-Cofund fellowship.

Notes and references

[a] *Department of Material and Life Science, Graduate School of Engineering, Osaka University, Suita, Osaka 565-0871, Japan*
E-mail: msupur@gmail.com
[b] *Graduate School of Engineering, Osaka University, Suita, Osaka 565-0871, Japan*
[c] *The Institute of Scientific and Industrial Research (SANKEN), Osaka University, 8-1 Mihoga-oka, Ibaraki, Osaka, 567-0047, Japan*
[d] *Aarhus Institute of Advanced Studies (AIAS), Aarhus University, Høegh-Guldbergs Gade 6B, 8000, Aarhus C, Denmark*
[e] *Interdisciplinary Nanoscience Center (iNANO), Aarhus University Gustav Wieds Vej 14, 8000, Aarhus C, Denmark*
[f] *Leibniz Institute für Molekulare Pharmakologie (FMP), NMR Supported Structural Biology, Robert Roessle Str. 10, 13125, Berlin, Germany*
† Electronic Supplementary Information (ESI) available: Additional figures (Fig. S1-S8). See DOI: 10.1039/b000000x/

1 (a) S. Toksoz, H. Acar and M. O. Guler, *Soft Matter*, 2010, **6**, 5839–5849T; (b) T. Aida, E. W. Meijer and S. I. Stupp, *Science*, 2012, **335**, 813–817; (c) S. Yagai, *Bull. Chem. Soc. Jpn.*, 2015, **88**, 28–58.
2 (a) F. Würthner, *Chem. Commun.*, 2004, 1564–1579; (b) M. R. Wasielewski, *Acc. Chem. Res.*, 2009, **42**, 1910–1921.
3 (a) L. Zang, Y. Che and J. S. Moore, *Acc. Chem. Res.*, 2008, **41**, 1596–1608; (b) M. Supur and S. Fukuzumi, *ECS J. Solid State Sci. Technol.*, 2013, **2**, M3051–M3062.
4 (a) S.-G. Chen, H. M. Branz, S. S. Eaton, P. C. Taylor, R. A. Cormier and B. A. Gregg, *J. Phys. Chem. B*, 2004, **108**, 17329–17336; (b) M. Supur, Y. Yamada, M. E. El-Khouly, T. Honda and S. Fukuzumi, *J. Phys. Chem. C*, 2011, **115**, 15040–15047; (c) M. Supur and S. Fukuzumi, *J. Phys. Chem. C*, 2012, **116**, 23274–23282; (d) K. V. Rao and S. J. George, *Chem.–Eur. J.*, 2012, **18**, 14286–14291; (e) M. Supur and S. Fukuzumi, *Phys. Chem. Chem. Phys.*, 2013, **15**, 2539–2546; (f) M. Supur, Y.-M. Sung, D. Kim and S. Fukuzumi, *J. Phys. Chem. C*, 2013, **117**, 12438–12445.
5 (a) Z. Chen, V. Stepanenko, V. Dehm, P. Prins, L. D. A. Siebbeles, J. Seibt, P. Marquetand, V. Engel and F. Würthner, *Chem.–Eur. J.*, 2007, **13**, 436–449; (b) Y. Che, A. Datar, X. Yang, T. Naddo, J. Zhao, L. Zhang, *J. Am. Chem. Soc.*, 2007, **129**, 6354–6355; (c) Y. Che, X. Yang, G. Liu, C. Yu, H. Ji, J. Zuo, J. Zhao and L. Zhang, *J. Am. Chem. Soc.*, 2010, **132**, 5743–5750; (d) S. Roy, D. K. Maiti, S. Panigrahi, D. Basak, A. Banerjee, *RSC Adv.*, 2012, **2**, 11053–11060; (e) Y. Huang, L. Fu, W. Zou and F. Zhang, *New. J. Chem.*, 2012, **36**, 1080–1084; (f) Y. Huang, W. Zhang, H. Zhai and C. Li, *J. Mater. Chem. C*, 2015, **3**, 466–472.
6 (a) D. M. de Leeuw, M. M. J. Simenon, A. R. Brown and R. E. F. Einerhand, *Synt. Met.*, 1997, **87**, 53–59; (b) A. P. Kulkarni, C. J. Tonzola, A. Babel and S. A. Jenekhe, *Chem. Mater.*, 2004, **16**, 4556–4573.
7 E. Dobruchowska, T. Marszalek and J. Ulanski, *Thin Solid Films*, 2014, **564**, 361–366.
8 Y. Huang, B. Quan, Z. Wei, G. Liu and L. Sun, *J. Phys. Chem. C*, 2009, **113**, 3929–3933.
9 (a) K. Masuda, H. Kaji and F. Horii, *Polym. J.*, 1999, **31**, 105–107; (b) K. Masuda, H. Kaji and F. Horii, *Polym. J.*, 2001, **33**, 190–198.
10 T. Shiga, Y. Hirose, A. Okada and T. Kurauchi, *J. Appl. Polym. Sci.*, 1992, **44**, 249–253.
11 (a) Y.-H. Yang, M. Haile, Y. T. Park, F. A. Malek and J. C. Grunlan, *Macromolecules*, 2011, **44**, 1450–1459; (b) H. Huang, W. Li, H. Wang, X. Zeng, Q. Wang and Y. Yang, *ACS Appl. Mater. Interfaces*, 2014, **6**, 1595–1600; (c) F. Xiang, S. M. Ward, T. M. Givens and J. C. Grunlan, *ACS Macro Lett.*, 2014, **3**, 1055–1058; (d) F. Xiang, S. M. Ward, T. M. Givens and J. C. Grunlan, *Soft Matter*, 2015, **11**, 1001–1007.
12 a) K. Petrak, *J. Appl. Polym. Sci.*, 1979, **23**, 2365–237; (b) K. Petrak and E. Pitts, *J. Appl. Polym. Sci.*, 1980, **25**, 879–886.
13 (a) C. A. Jolly and J. R. Reynolds, *Chem. Mater.*, 1990, **2**, 479–480; (b) W. F. Stickle, J. R. Reynolds and C. A. Jolly, *Langmuir*, 1991, **7**, 2460–2463; (c) L. L. Miller, C. Zhong and Y. Hong, *Synt. Met.*, 1994, **62**, 71–73; (d) Y. Hong, M. E. Benz and L. L. Miller, *Synt. Met.*, 1995, **68**, 281–286.
14 F. Donati, A. Pucci and G. Ruggeri, *Phys. Chem. Chem. Phys.*, 2009, **11**, 6276–6282.
15 C. Tozlu, S. Erten-Ela, Th. B. Singh, N. S. Sariciftci and S. Içli, *Synt. Met.*, 2013, **172**, 5–10.
16 H. J. Salavagione, G. Martinez, R. Gomez and J. L Segura, *J. Polym. Sci., Part A: Polym. Chem.*, 2010, **48**, 3613–3622.
17 (a) C. Karapire, C. Zafer and S. Içli, *Synt. Met.*, 2004, **145**, 51–60; (b) T. Tang, J. Qu, K. Müllen and S. E. Webber, *Langmuir*, 2006, **22**,

7610–7616; (c) F. Donati, A. Pucci, C. Cappeli, B. Mennucci and G. Ruggeri, *J. Phys. Chem. B.*, 2008, **112**, 3668–3679; (d) T. A. Everett and D. A. Higgins, *Langmuir*, 2009, **25**, 13045–13051; (e) N. Jouault, Y. Xiang, E. Moulin, G. Fuks, N. Giuseppone and E. Buhler, *Phys. Chem. Chem. Phys.*, 2012, **14**, 5718–5728; (f) F. Ciardelli, G. Ruggeri and A. Pucci, *Chem. Soc. Rev.*, 2013, **42**, 857–870; (g) E. Dahan and P. R. Sundararajan, *Soft Matter*, 2014, **10**, 5337–5349; (h) S. K. Nisha and S. K. Asha, *ACS Appl. Mater. Interfaces*, 2014, **6**, 12457–12466; (i) E. Dahan and P. R. Sundararajan, *Eur. Polym. J.*, 2015, **65**, 4–14.

18 The PVA films with high TAIPDI contents (10 wt.% and more) were homogenous to the eye but inhomogenity appears at low TAIPDI ratios depending on the drying duration.

19 (a) S. U. Celik, U. Akbey, A. Bozkurt, R. Graf and H. W. Spiess, *Macromol. Chem. Phys.*, 2008, **209**, 593–603; (b) S. U. Celik, U. Akbey, R. Graf, A. Bozkurt and H. W. Spiess, *Phys. Chem. Chem. Phys.*, 2008, **10**, 6058–6066; (c) U. Akbey, R. Graf, Y. G. Peng, P. P. Chu and H. W. Spiess, *J. Polym. Sci., Part B: Polym. Phys.*, 2009, **47**, 138–155; (d) A. Sezgin, U. Akbey, R. Graf, A. Bozkurt and A. Baykal, *J. Polym. Sci., Part B: Polym. Phys.*, 2009, **47**, 1267–1274; (e) U. Akbey, R. Graf, P. P. Chu and H. W. Spiess, *Aust. J. Chem.*, 2009, **62**, 848-856; (f) U. Akbey, S. Granados-Focil, E. B. Coughlin, R. Graf and H. W. Spiess, *J. Phys. Chem. B*, 2009, **113**, 9151–9160; (g) V. Percec, M. Peterca, T. Tadjiev, X. Zeng, G. Ungar, P. Leowanawat, E. Aqad, M. R. Imam, B. M. Rosen, U. Akbey, R. Graf, S. Sekharan, D. Sebastiani, H. W. Spiess, P. A. Heiney and S. D. Hudson, *J. Am. Chem. Soc.*, 2011, **133**, 12197–12219.

20 (a) S. P. Brown, *Macromol. Rapid Commun.*, 2009, **30**, 688–716; (b) S. P. Brown, *Solid State Nucl. Mag. Res.*, 2012, **41**, 1–27.

21 Formation radical anions of TAIPDI in PVA films was confirmed by the EPR measurements (Fig. S4, ESI).

22 Formation of the reduced species was not explicitly observed when TAIPDI, cast on a glass substrate from aqueous solution without PVA, was exposed to hydrazine vapour (Fig. S5, ESI).

23 (a) R. O. Marcon and S. Brochsztain, *J. Phys. Chem. A*, 2009, **113**, 1747–1752; (b) L. Zhong, F. Xing, W. Shi, L. Yan, L. Xie and S. Zhu, *ACS Appl. Mater. Interfaces*, 2013, **5**, 3401–3407.

24 The same decay profiles were obtained at the different wavelengths of the UV-Vis spectrum.

25 The currents are the average values of 15-20 *I-V* measurements performed on the different regions of the corresponding film spot. For the *I-V* curve of neat PVA film, see: Fig. S7, ESI.

26 To calculate the conductivity, it was assumed that the flow of electric current occurred in the shortest distance between (50-60 μm) two electrodes, having a diameter of 10 μm.